Tracking cosmic-ray spectral variations with neutron monitor time-delay measurements at high cutoff rigidity during 2007-2017

C. Banglieng[a,b], **D. Ruffolo**[*a], **A. Sáiz**[a], **P. Evenson**[c], **T. Nutaro**[d]

[a]*Department of Physics, Faculty of Science, Mahidol University, Bangkok 10400, Thailand.*
[b]*National Astronomical Research Institute of Thailand (NARIT), Chiang Mai 50180, Thailand.*
[c]*Bartol Research Institute, Department of Physics and Astronomy, University of Delaware, Newark, DE 19716, USA.*
[d]*Department of Physics, Faculty of Science, Ubon Ratchathani University, Ubon Ratchathani 34190, Thailand.*
 E-mail: bchanoknan@gmail.com, david.ruf@mahidol.ac.th, alejandro.sai@mahidol.ac.th, evenson@udel.edu, tnutaro@yahoo.com.

We present measurements of the leader fraction of neutron monitor counts that did not follow other counts in the same counter tube from the same cosmic ray shower. We use time-delay histograms collected at the Princess Sirindhorn Neutron Monitor at Doi Inthanon, Thailand, which has the world's highest vertical cutoff rigidity for a fixed station (16.8 GV). Changes in the leader fraction are a precise indicator of cosmic ray spectral variations above the cutoff. Our data set from 2007 to 2017 spans a full cycle of solar modulation, including the all-time cosmic ray maximum of 2009 and minimum near the end of 2014, the count rate now having returned to its initial value. The electronics to collect time-delay histograms have been upgraded twice, and we have corrected for such changes to develop a long-term leader fraction dataset. We examine the spectral variation of Galactic cosmic rays above ∼17 GV resulting from solar modulation and its solar magnetic polarity dependence.

35th International Cosmic Ray Conference
*12-20 July, 2017*
Bexco, Busan, Korea

---

*Speaker.

1. Introduction

Neutron monitors (NMs) are ground-based detectors of secondary neutrons from interactions of primary cosmic rays in Earth's atmosphere. With high count rates and stable operation, NMs have precisely tracked variations in the flux of Galactic cosmic rays (GCRs) for decades and perform key measurements of solar modulation, i.e., variations with the roughly 11-year sunspot cycle [4] and 22-year solar magnetic cycle [5]. Solar modulation is scientifically interesting because the GCRs traverse the heliosphere on their way to Earth and provide remote sensing of heliospheric propagation conditions relating to the turbulent solar wind and interplanetary magnetic field.

Solar modulation is strongly energy-dependent [9], and a disadvantage of ground-based measurements is that the primary cosmic ray energy is not directly measured. The energy response of an NM can be controlled to some extent by its location on Earth's surface, using Earth itself as a magnetic spectrometer. For a given location and particle arrival direction there is a rather sharp geomagnetic cutoff in rigidity (momentum per charge) below which particles cannot reach Earth's atmosphere. The effective geomagnetic cutoff for vertically arriving particles varies from ∼17 GV in and near Thailand to <0.01 GV in some polar regions; for low geomagnetic cutoff, there is also an atmospheric cutoff at ∼1 GV, which is the threshold for primary cosmic rays to produce atmospheric secondaries detected by the NM at ground level. Therefore, while NM count rates track the GCR flux, the worldwide NM network also provides some information on GCR spectral variations in an intermediate rigidity range when comparing count rates at different cutoff rigidities. However, although individual NM count rate measurements can have high statistical precision, there are various uncertainties involved with comparing long-term data from different locations. These include the strong dependence of the NM yield function on the altitude of the station and also effects of different NM configurations, electronic dead time, structures surrounding the stations, seasonal effects, and atmospheric structure [1, 7, 8], as well as long-term drifts [12].

Figure 1: Example of time delay histograms collected for one neutron counter tube in the PSNM at Doi Inthanon during one hour. (a) Long time delays follow an exponential distribution (red) as expected for unrelated neutron detection events. (b) At short time delays (< 2 ms), the distribution deviates substantially from that exponential because many counts are associated other counts due to the same primary cosmic ray. The hashed region indicates the dead time of the time delay histogram, t_d. From histograms such as these, we extract the leader fraction L of neutrons that did not follow a previous neutron detected in the same tube from the same cosmic ray, and L serves as an indicator of the spectral index of primary cosmic rays.
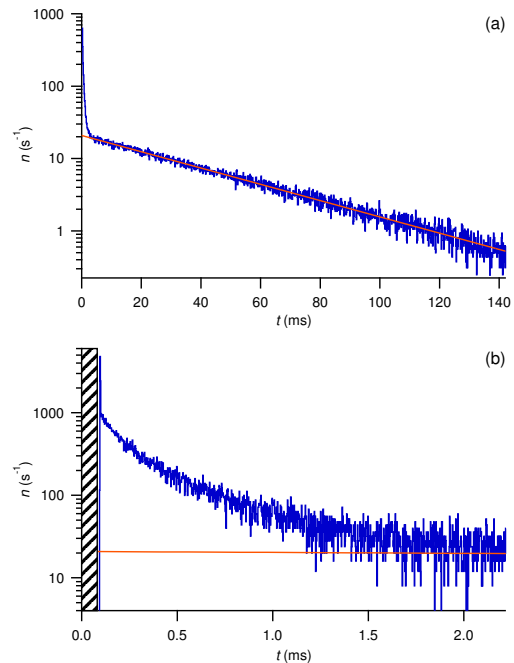
For these reasons, we have developed a capability to precisely track spectral variations using data from a single NM station. We built specialized electronics to record neutron time-delay histograms [3], and an example of the resulting time-delay histograms is shown in Figure 1. We also developed analysis techniques to remove the effect of chance coincidences and extract the "leader fraction" L of neutron monitor counts that did not follow other counts in the same counter tube from the same cosmic ray shower [13]. Data from latitude surveys with a ship-borne NM during 2001-2007 show that L varies with cutoff rigidity in the manner expected from Monte Carlo simulations [8], confirming that variations in L indicate variations in the primary cosmic ray spectrum. The first fixed NM station where these electronics were used is the Princess Sirindhorn Neutron Monitor (PSNM) at Doi Inthanon, Thailand, which has the world's highest cutoff rigidity for a fixed station (vertical cutoff $\approx$ 16.8 GV). Here we present a long-term dataset of the leader fraction at Doi Inthanon from 2007 December to 2017 June, which spans a full cycle of solar modulation, including the all-time cosmic ray maximum of 2009 and minimum near the end of 2014, the count rate now having returned to its initial value. While comparisons of NM count rates provide spectral information over rigidities within the worldwide range of cutoff rigidities, the leader fraction at Doi Inthanon indicates spectral variations at a rigidity beyond the Earth's maximum cutoff.

2. Analysis of Neutron Time-Delay Histograms

2.1 Observations at Doi Inthanon, Thailand

PSNM is located at the summit of Doi Inthanon, Thailand's highest mountain, at longitude 18.59°N, longitude 98.49°E, and altitude 2560 m. It employs 18 neutron detectors (^{10}BF$_3$ proportional counter tubes) in the standard NM64 design (i.e., an 18NM64 configuration) with all tubes individually surrounded lead producer and arranged in a continuous single row inside the polyethylene reflector. Over the solar modulation cycle, the total count rate ranges from about 605 to 625 Hz, corresponding to 2.18 to 2.25 million counts per hour. Details about the detector can be found in [13].

Our specialized electronics that output histograms of the time delays between successive neutron detections in the same counter tube [3] were first implemented on a series of latitude surveys from 2000 to 2007 [8]. Similar systems have been developed by other groups (e.g., [2, 6]). The first use of our electronics at a fixed station was at PSNM since the start of operations in 2007 August. Here we analyze data taken since 2007 December 9, the start of operations with the complete set of 18 counter tubes.

Table 1 details the evolution of the firmware in the electronics and the software in the data acquisition system used to collect time delay histograms at PSNM. We refer to the firmware originally implemented as the 600 series. We originally collected daily time-delay histograms, and then changed to hourly histograms on 2009 June 29. The 600 series collected only 16 time delays per s per tube, resulting in the "first-pulse bias" described by [13]. Then we upgraded to the 700 series on 2011 Jan 15, allowing almost all time delays (at $\approx$34 Hz per tube) to be collected for improved statistics. We upgraded to the 800 series on 2014 Jun 11 in order to record absolute times and calculate cross-tube time delays (see [14]), which are not used in the present analysis. The 800 series firmware also reduced the time-delay dead time for improved collection of time-delay

Table 1: Time periods of leader fraction data collection from the 18NM64 at Doi Inthanon, Thailand.

Time period	Start date	End date	Cadence	Firmware series (Number of tubes)	Software version[a]
1	2007 Dec 9	2009 Jun 28	Daily	600 (18)	—
1	2009 Jun 29	2011 Jan 15	Hourly	600 (18)	—
2	2011 Jan 15	2014 Feb 8	Hourly	700 (18)	—
3	2014 Feb 8	2014 Jun 11	Hourly	700 (17)	—
4	2014 Oct 17	2015 Mar 3	Hourly	800 (18)	8.46-8.47
5	2015 Mar 3	2015 May 31	Hourly	800 (18)	8.50
6	2015 May 31	2016 Jun 30	Hourly	600 (6), 800 (12)	8.50-8.82
7	2016 Jun 30	2017 Jun 7	Hourly	800 (18)	8.82

[a] Only relevant for 800 series firmware.

data (note that the dead time related to the count rate was never changed). Starting with the 800 series, time delays are calculated by the data acquisition software. The software version changes that affected the time-delay histograms are indicated in Table 1. The 800 series data did not yield a useful estimate of the leader fraction from 2014 June to 2014 October while the software was under development. Note that there were no changes to the circuitry used for count rate data, which were collected continuously from the 18NM64 since 2007 December.

Note that our electronics to record time-delay histograms have more recently been implemented at other fixed NM stations: at the South Pole (on 1 NM tube since 2014 January, then later on all 3 NM tubes), at McMurdo, Antarctica (on 6 tubes from 2015 January until the station closed on 2017 January 7), at Newark, USA (on 3 tubes since 2015), and at Jang Bogo, Antarctica (on all 5 tubes since 2015 December). Those data will be analyzed in further work.

2.2 Extraction of the Leader Fraction

As shown in Figure 1, at long time delays the histograms are dominated by chance coincidences, which strongly affect traditional measures of multiplicity in a fixed time window. Therefore, [13] developed methods to statistically remove the effect of chance coincidences to extract the leader fraction *L*. This is defined as the fraction of neutron counts that did not follow another count in the same tube due to the same primary cosmic ray, i.e., did not follow another count in the same tube with a short time delay that is not consistent with chance coincidence. Statistically, more energetic primary cosmic rays lead to more energetic secondary particles that produce more neutrons when interacting inside the neutron monitor (typically in the lead producer), which can then be detected as sequences of more counts in the same tube with shorter time delays. Thus a harder cosmic ray spectrum with a lower spectral index leads to a lower leader fraction. Ref. [13] showed that the leader fraction at Doi Inthanon can indicate short-term spectral variations; the present work extends that to determine a long-term time series of *L* for the study of solar modulation.

Ref. [13] described three methods for determining L, and implemented the first (Method 1). However, in the present work, when comparing data from different software versions, we find that Method 2 is more robust under such changes, perhaps because it uses short time delays more than long time delays, and we now use Method 2.

2.3 Normalization and Correction of the Leader Fraction

To interpret long-term variation of the leader fraction, we have normalized for version changes in the electronics and data acquisition, and developed corrections of L (for Method 2) for variations of pressure and water vapor.

Note that NM count rates are essentially always corrected for pressure variation, and at the tropical location of Doi Inthanon, correction for water vapor is necessary when studying bare counter rates and the leader fraction [13]. [It even affects the count rate, with a peak-to-peak seasonal variation of 0.3% [9], but we do not correct the count rate for water vapor in the present work.] Those works described corrections based on the surface water vapor pressure E_w at Doi Inthanon as calculated from the Global Atmospheric Data Assimilation (GDAS) database (see http://ready.arl.noaa.gov/gdas1.php). In particular, [13] found a nonlinear relationship between pressure-corrected L and E_w, which they modeled using power-law relationships. Here we have integrated over the atmospheric model to estimate the integrated water vapor I as a function of time. When examining data from each individual tube using the 700 series electronics, we find a nearly linear relationship between pressure-corrected L and I. Our interpretation is that the leader fraction, which mainly responds to sub-GeV secondary neutrons from the atmospheric cascades of cosmic rays [8], has a small effect from water vapor throughout the atmosphere that is nearly linear in I. The surface water vapor E_w can serve as a proxy for I but often saturates during the rainy season (with nearly 100% relative humidity), so that L has a nonlinear relationship with E_w. In that case, I should provide a more accurate measure of water vapor content for correcting L at Doi Inthanon.

Each counter tube has a different value of L, mainly due to its position and electronic dead time [13]. We first normalized L from each tube to a standard set of tubes based on statistics of measured L ratios. These ratios were independent of the firmware and software version, though on 2014 Dec 7 we swapped the end tubes 1 and 18, requiring separate normalizations of the end tubes before and after that time. After that normalization, L was averaged over all tubes that provided good data. An overall normalization for each normalization period in Table 1 was directly determined from calibration periods when we simultaneously operated different firmware versions on different sets of tubes for a statistical comparison, or by matching the time series before and after a transition.

3. Long-Term Variation of the Leader Fraction

Figure 2 shows preliminary results for the corrected and normalized leader fraction L from the 18NM64 at Doi Inthanon, Thailand from 2007 December to 2017 June, as well as the count rate C over that time. The count rate shows solar modulation over a complete cycle, having increased to the time of the highest GCR flux of the Space Age in 2009 [11, 10, 12], decreased to a cosmic ray minimum in 2014, and now increased back above its starting value. Figure 3 shows trimester (three-month) averaged data for L vs. C over the same time period. Numerical labels indicate the
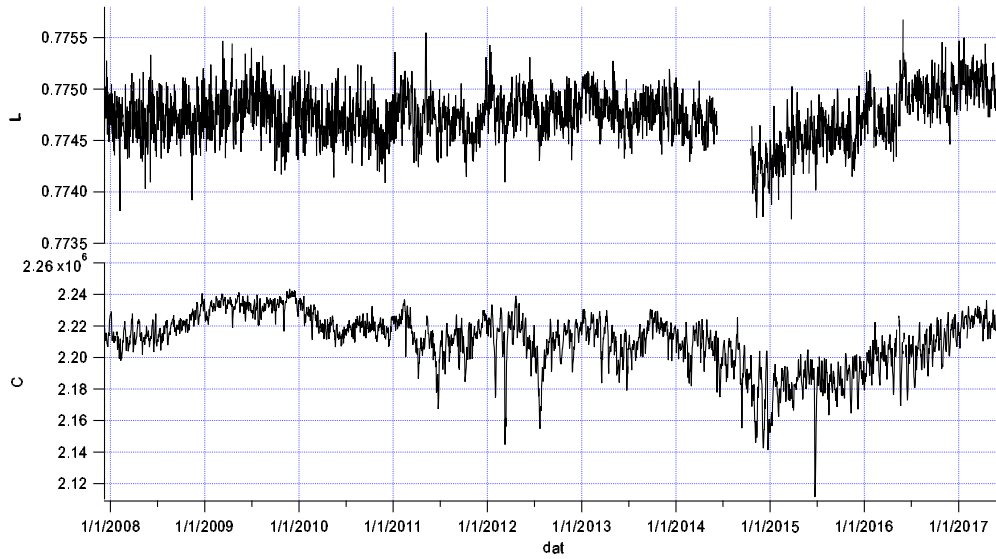
Figure 2: Preliminary results for the leader fraction *L* (upper panel) and count rate *C* (lower panel, in counts per hour) vs. time in the 18NM64 at Doi Inthanon, Thailand at vertical cutoff rigidity ≈ 16.8 GV during 2007-2017. The near constancy of *L*, an indicator of spectral variation well above the cutoff, indicates that during the period surrounding the record-high cosmic ray peak of 2009, the solar modulation extended up to much higher rigidity than the cutoff. After the cosmic ray minimum in 2014, *L* varied in tandem with *C*, indicating that solar modulation did not extend far above the cutoff.
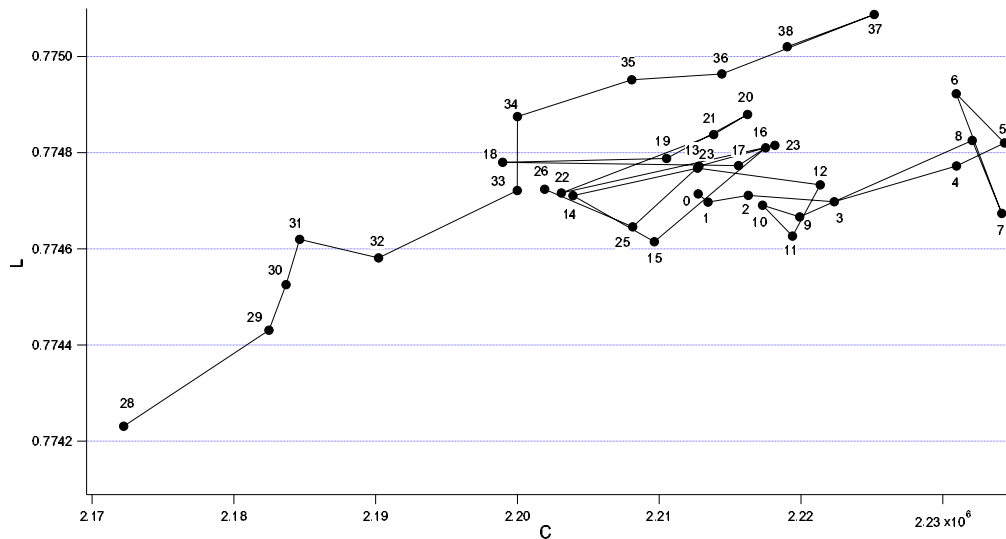

Figure 3: Preliminary results for trimester (three-month) averages of the leader fraction *L* vs. count rate *C* (in counts per hour) in the 18NM64 at Doi Inthanon during 2007-2017. Labels indicate the time period, starting at 0 for the last trimester of 2007 and ending at 38 for the second trimester of 2017. The hysteresis indicates that for solar modulation over this period, the spectrum did not "roll" down and "unroll" back up in the same way.

6

time period, starting at 0 for the last trimester of 2007 and ending at 38 for the second trimester of 2017.

Note that *L* serves as a measure of the GCR spectral index at rigidities substantially above the cutoff rigidity of ≈17 GV (i.e., increasing *L* implies a lower multiplicity and a softer spectrum), while *C* measures the GCR flux just above the cutoff [8]. How might we expect *L* to vary with solar modulation? A basic concept of solar modulation is that the cosmic ray spectrum "rolls" downward from the local interstellar spectrum (LIS) and then "unrolls" back up again. The change in the spectrum is much greater at low rigidity, while at sufficiently high rigidity there is almost no solar modulation. Thus we expect that *L* should increase with increasing *C*, as the GCR spectrum unrolls to the softer LIS. The widely used range of models with a single modulation parameter assume that the spectrum always rolls and unrolls with the same spectral shape. From such models, we would expect *L* vs. *C* to move along a constant track. Any substantial hysteresis (deviation from a prior track) cannot be explained by a model with a single modulation parameter.

From Figures 2 and 3, we can roughly divide the dataset into three modulation periods. From 2007 December to 2010 December (trimesters 0 to 12), *C* varied significantly but *L* was roughly constant with minor variations. This corresponds to a horizontal band in Figure 3. Physically, if the flux varies without significant spectral variation, that implies that the GCR spectrum was rising and falling without much change in spectral index. In other words, the solar modulation extended to rigidities much higher than the cutoff.

During the second modulation period, from 2011 January to 2014 June (trimesters 13 to 26), both *L* and *C* stayed in the same range with some fluctuations, including Forbush decreases, which have not been removed in the present analysis. ([13] showed that some but not all Forbush decreases in *C* are also accompanied by decreases in *L*.) This corresponds to a special 4-year plateau in *C* at Doi Inthanon, corresponding to the time when the heliospheric current sheet tilt angle ≳ 50°, a plateau was not observed in NM at low cutoff rigidity [9]. The weak variation of *L* confirms that there was little systematic change in modulation conditions during this time period above the Doi Inthanon cutoff rigidity of about 17 GV. During this time there was a change in solar magnetic polarity.

After trimester 27 when the time delay histograms were not usable, we observed a third modulation period from 2014 October to 2017 June (trimesters 28 to 38), i.e., to the end of our analysis period, in which *C* and *L* increased in tandem from their solar-cycle minimum values. Interestingly, *L* reached a higher value in 2017 than during the record-high GCR maximum of 2009, indicating an even softer spectrum in 2017. When *L* changes strongly together with *C*, this indicates a strong change in the spectrum over rigidities above the cutoff, implying that the spectral change due to modulation in this period was concentrated at rigidities slightly above the cutoff, with much less change at rigidities well above the cutoff. In other words, the solar modulation did not extend far above the cutoff, in contrast with the first modulation period.

This third period has a nearly linear track in *L* vs. *C* that is not consistent with the horizontal track during 2007 December to 2010 September. The intermediate second modulation period, in which neither *L* or *C* varied systematically over about 4 years, is at a region of the *C-L* plane that could be assigned to either track. The existence of two distinct tracks in this plane cannot be explained by models with a single modulation parameter. These results serve as yet another example of a difference in solar modulation after a change in solar magnetic polarity. We see that the leader

fraction inferred from time-delay histograms at Doi Inthanon provides new information on solar modulation above ~ 20 GV, extending the rigidity range of information from the worldwide NM network.

Acknowledgments

References

[1] Aiemsa-ad, N., Ruffolo, D., Sáiz, A., et al. 2015, JGRA, 120, 5253

[2] Balabin, Yu. V., Gvozdevsky, B. B., Vashenyuk, E. V., & Schur, L. I. 2008, Proc. 30th ICRC (Mérida), 1, 257

[3] Bieber, J. W., Clem, J. M., Duldig, M. L., et al. 2004, ApJ, 601, L103

[4] Forbush, S. E. 1954, JGR, 59, 525

[5] Jokipii, J. R., & Thomas, B. 1981, ApJ, 243, 1115

[6] Kollár, V., Kudela, K., & Minarovjech, M. 2011, Contrib. Astron. Obs. Skalnaté Pleso, 41, 5

[7] Mangeard, P.-S., Ruffolo, D., Sáiz, A., Madlee, S., & Nutaro, T. 2016a, JGRA, 121, 743

[8] Mangeard, P.-S., Ruffolo, D., Sáiz, A., et al. 2016b, JGRA, 121, 11620

[9] Mangeard, P.-S., Clem, J., Evenson, P., et al., these proceedings

[10] McDonald, F. B., Webber, W. R., & Reames, D. V. 2010, GRL, 37, L18101

[11] Mewaldt, R. A., Davis, A. J., Lave, K. A., et al. 2010, ApJL, 723, L1

[12] Oh, S., Bieber, J. W., Evenson, P., et al. 2013, JGRA, 118, 5431

[13] Ruffolo, D., Sáiz, A., Mangeard, P.-S., et al. 2016, ApJ, 817, 38

[14] Sáiz, A., Mitthumsiri, W., Ruffolo, D., Evenson, P., & Nutaro., T, these proceedings